PERGAMON

Applied Geochemistry 15 (2000) 1291–1305

Applied Geochemistry

www.elsevier.com/locate/apgeochem

Influence of anthropogenic activity on the lead isotope signature of Thau Lake sediments (southern France): origin and temporal evolution

F. Monna[a, b,*], N. Clauer[c], T. Toulkeridis[c, d], J.R. Lancelot[a]

[a]*Laboratoire de Géochimie Isotopique, Université de Montpellier, Place E. Bataillon, F-34095, Montpellier, France*
[b]*Institut FA Forel, 10 route de Suisse, CH-1290, Versoix, Switzerland*
[c]*Centre de Géochimie de la Surface (ULP–CNRS), Ecole et Observatoire des Sciences de la Terre, 1 rue Blessig, F-67084, Strasbourg, France*
[d]*Institut für Geologie, Fachbereich Geowissenschaften, Universität Mainz, 55099, Mainz, Germany*

Received 24 November 1998; accepted 5 November 1999
Editorial handling by P. Fritz

Abstract

Lead concentrations and isotopic compositions were determined on both bulk sediments deposited in the Thau lake in southern France during the last 200 years, and leachates derived from a series of sequential leachings of the sediments, making it possible to identify the sources, natural (i.e. indigenous lithologic) or anthropogenic, and to quantify the different inputs of Pb.

Two distinct inputs of Pb could be distinguished. One of these corresponds to the terrigenous material entering the basin, representative of the local natural Pb 'background'. Its supply remained steady most of the time with $^{206}Pb/^{207}Pb$ ratios of 1.200 ± 0.003, except at the time of heavy storms producing voluminous and sudden depositions, such as that of September 1875. This Pb supply is mainly hosted by the detrital silicate fraction of the sediments. The second Pb input is a direct consequence of anthropogenic activities of various industrial and domestic emissions in the region, particularly due to the city of Sète and, to a lesser extent, to the villages in the watershed. The $^{206}Pb/^{207}Pb$ ratios of this input are of 1.142–1.162. The Pb added to gasoline could also be identified in the uppermost sediments, because of its specific $^{206}Pb/^{207}Pb$ ratios of 1.069–1.094. The leaching experiments also showed that the anthropogenic Pb is mainly hosted by the oxi-hydroxides of the sediments and to a lesser extent by the carbonates. It may also be adsorbed on particle surfaces, while only limited amounts are bound to organic matter.

1. Introduction

Impact of human activity and its temporal evolution have been extensively studied in marine or lacustrine ecosystems (e.g. Véron et al., 1987; Wahlen and Thompson, 1980; Zwolsman et al., 1993). These studies underlined the fact that Pb concentrations alone are

* Corresponding author. Géosol UMR–INRA, CST, Université de Bourgogne, 6 bd Gabriel, F-21000 Dijon, France. Fax: +33-3-80-39-63-87.
E-mail address: fabrice.monna@u-bourgogne.fr (F. Monna).

0883-2927/00/$ - see front matter
PII: S0883-2927(99)00117-1

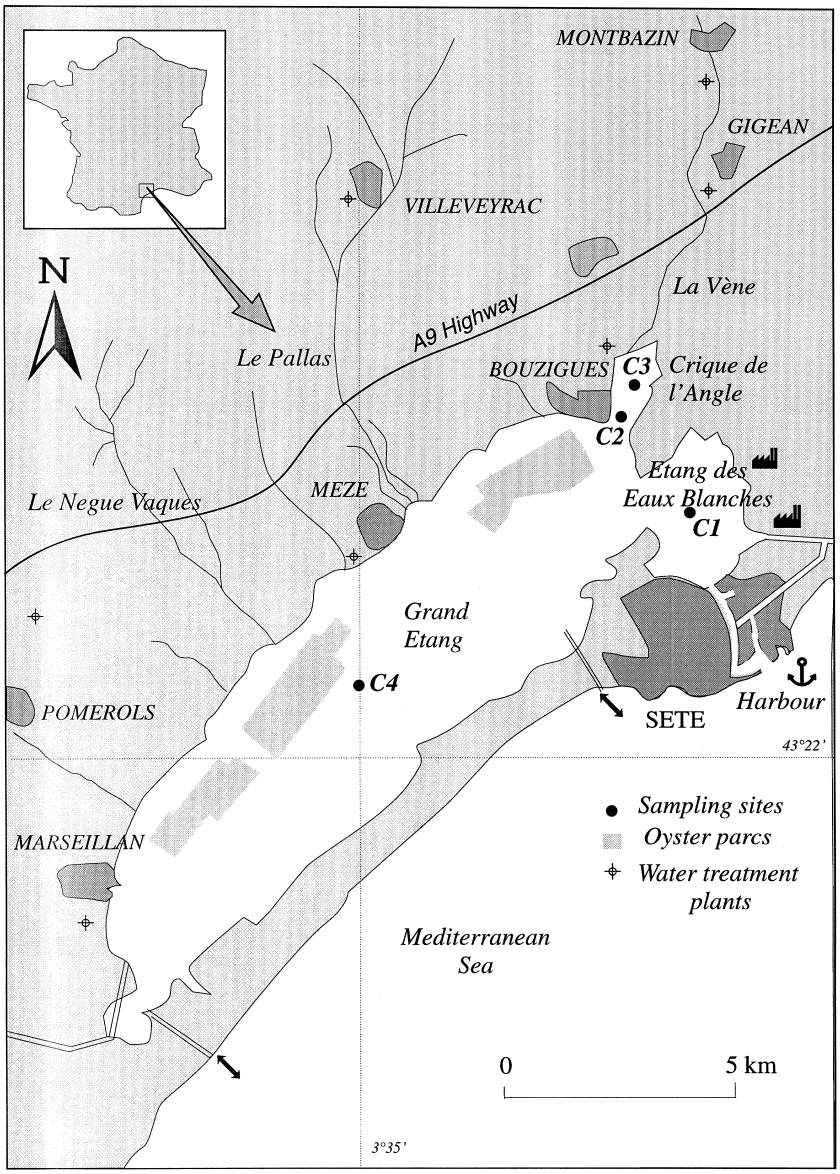

Fig. 1. Map of the Thau basin with the sampling locations.

not helpful to detail the impact of anthropogenic Pb in such varied ecosystems, as concentrations by themselves cannot elucidate the origin of the Pb. Accurate identification of specific contamination is often difficult, but Pb isotope geochemistry can provide crucial information (1) on identification of the Pb provenance (e.g. Doe, 1970; Kramers and Tolstikhin, 1997 and the special 1994 issue of Geochim. Cosmochim. Acta dedicated to Clair C. Patterson), and (2) on broad definition of the classes of pollutant products. For instance, it has been demonstrated that present-day anthropogenic Pb can be divided into two generic groups in Western Europe: leaded gasoline and the Pb emitted by industrial plants (Elbaz-Poulichet et al., 1984, 1986; Hamester et al., 1994; Monna et al., 1997b; Sudgen et al., 1993). Both are significantly different from local bedrock signatures, because the anthropogenic Pb generally derives from remote ore deposits characterised by low radiogenic signatures.

In the natural ecosystem of the Thau coastal basin, part of the Pb incorporated in the sediments derives from outcropping soils and rocks, and any remaining Pb results from various anthropogenic sources such as the anti-knock agent added to gasoline, industrial and

Table 1
Pb isotopic compositions of the untreated bulk sediments

Depth (cm)	$^{206}Pb/^{204}Pb$	2σ	$^{207}Pb/^{204}Pb$	2σ	$^{208}Pb/^{204}Pb$	2σ	$^{206}Pb/^{207}Pb$	2σ	$^{208}Pb/^{206}Pb$	2σ
Core C1										
0–1	18.290	0.006	15.612	0.007	38.23	0.02	1.1716	0.0001	2.0902	0.0003
1.0–2.2	18.362	0.003	15.673	0.003	38.50	0.01	1.1717	0.0001	2.0968	0.0003
2.2–3.4	18.411	0.005	15.679	0.005	38.53	0.01	1.1742	0.0001	2.0929	0.0003
3.4–4.6	18.417	0.003	15.637	0.003	38.44	0.01	1.1780	0.0001	2.0871	0.0002
4.6–5.8	18.409	0.005	15.630	0.005	38.45	0.02	1.1778	0.0001	2.0885	0.0003
5.8–7.0	18.433	0.004	15.668	0.004	38.60	0.01	1.1765	0.0001	2.0956	0.0003
7.0–8.5	18.395	0.003	15.635	0.004	38.44	0.01	1.1765	0.0001	2.0897	0.0003
8.5–9.5	18.421	0.012	15.675	0.011	38.62	0.03	1.1751	0.0001	2.0970	0.0004
9–5–11.0	18.388	0.005	15.625	0.005	38.42	0.02	1.1769	0.0001	2.0893	0.0003
11–12.5	18.386	0.012	15.638	0.011	38.53	0.03	1.1757	0.0001	2.0956	0.0005
12.5–13.8	18.431	0.006	15.633	0.006	38.53	0.02	1.1790	0.0001	2.0904	0.0003
13.8–15	18.488	0.003	15.659	0.011	38.53	0.01	1.1807	0.0001	2.0870	0.0003
15–16.2	18.474	0.005	15.645	0.005	38.61	0.01	1.1808	0.0001	2.0901	0.0003
♯15–16.2	18.469	0.007	15.643	0.007	38.57	0.02	1.1806	0.0001	2.0885	0.0003
16.2–17.4	18.585	0.006	15.677	0.005	38.77	0.02	1.1854	0.0001	2.0859	0.0003
♯16.2–17.4	18.606	0.005	15.698	0.005	38.74	0.02	1.1853	0.0001	2.0822	0.0003
17.4–18.5	18.606	0.014	15.649	0.012	38.63	0.03	1.1890	0.0001	2.0762	0.0004
18.5–20	18.624	0.007	15.687	0.007	38.77	0.02	1.1872	0.0001	2.0818	0.0003
20–21.5	18.550	0.009	15.625	0.008	38.56	0.02	1.1872	0.0001	2.0785	0.0004
21.5–23	18.535	0.003	15.634	0.003	38.52	0.01	1.1855	0.0001	2.0783	0.0003
23–24	18.538	0.011	15.659	0.010	38.67	0.03	1.1839	0.0001	2.0858	0.0004
♯23–24	18.552	0.018	15.667	0.017	38.70	0.04	1.1842	0.0002	2.0860	0.0005
26–27	18.484	0.006	15.641	0.006	38.60	0.02	1.1818	0.0001	2.0883	0.0003
31–32	18.455	0.012	15.614	0.011	38.46	0.03	1.1818	0.0001	2.0843	0.0003
36–37	18.693	0.003	15.667	0.004	38.70	0.01	1.1931	0.0001	2.0705	0.0003
Core C2										
0–1	18.272	0.003	15.666	0.003	38.46	0.01	1.1663	0.0001	2.1050	0.0003
1–2.2	18.263	0.008	15.589	0.007	38.24	0.02	1.1715	0.0001	2.0940	0.0003
2.2–3.4	18.383	0.003	15.684	0.004	38.61	0.01	1.1720	0.0001	2.1005	0.0005
3.4–4.6	18.352	0.003	15.689	0.003	38.55	0.01	1.1697	0.0001	2.1007	0.0003
4.6–6	18.427	0.006	15.691	0.006	38.62	0.02	1.1743	0.0001	2.0960	0.0004
6–7.2	18.531	0.006	15.682	0.006	38.63	0.02	1.1817	0.0001	2.0847	0.0003
7.2–8.4	18.589	0.004	15.663	0.004	38.72	0.01	1.1868	0.0001	2.0827	0.0003
♯7.2–8.4	18.599	0.006	15.673	0.006	38.73	0.02	1.1867	0.0001	2.0821	0.0003
♯♯7.2–8.4	18.623	0.007	15.671	0.007	38.73	0.02	1.1885	0.0001	2.0793	0.0003
8.4–9.6	18.588	0.004	15.635	0.004	38.57	0.01	1.1888	0.0001	2.0750	0.0003
9.6–10.8	18.650	0.011	15.702	0.010	38.86	0.03	1.1877	0.0002	2.0838	0.0004
10.8–12	18.543	0.010	15.675	0.009	38.72	0.03	1.1831	0.0001	2.0883	0.0003
13–14	18.599	0.006	15.707	0.006	38.80	0.02	1.1840	0.0001	2.0864	0.0004
♯13–14	18.597	0.022	15.704	0.020	38.79	0.06	1.1841	0.0003	2.0865	0.0006
16–17	18.636	0.020	15.707	0.017	38.84	0.04	1.1865	0.0002	2.0841	0.0005
20–21	18.656	0.009	15.690	0.008	38.76	0.02	1.1890	0.0001	2.0780	0.0003
♯20–21	18.647	0.004	15.687	0.004	38.76	0.01	1.1886	0.0001	2.0788	0.0003
21–22.5	18.630	0.008	15.671	0.007	38.76	0.02	1.1887	0.0001	2.0803	0.0003
26.5–27.5	18.776	0.005	15.687	0.005	38.82	0.02	1.1969	0.0001	2.0673	0.0003
32.5–33.5	18.654	0.003	15.679	0.004	38.72	0.01	1.1897	0.0001	2.0760	0.0003
40–41	18.697	0.015	15.710	0.013	38.85	0.04	1.1902	0.0002	2.0775	0.0004
50–51	18.697	0.026	15.666	0.023	38.69	0.06	1.1929	0.0004	2.0706	0.0008
56–57	18.696	0.012	15.677	0.010	38.78	0.03	1.1926	0.0004	2.0740	0.0008
62–63	18.721	0.003	15.682	0.004	38.84	0.01	1.1938	0.0001	2.0746	0.0004
♯62–63	18.686	0.014	15.643	0.013	38.69	0.03	1.1946	0.0002	2.0706	0.0003
68–69	18.743	0.010	15.682	0.009	38.81	0.03	1.1953	0.0001	2.0707	0.0004
♯68–69	18.754	0.006	15.708	0.006	38.89	0.02	1.1954	0.0001	2.0713	0.0004
78–79	18.730	0.005	15.697	0.005	38.86	0.02	1.1932	0.0001	2.0748	0.0003

(continued on next page)

Table 1 (*continued*)

Depth (cm)	$^{206}Pb/^{204}Pb$	2σ	$^{207}Pb/^{204}Pb$	2σ	$^{208}Pb/^{204}Pb$	2σ	$^{206}Pb/^{207}Pb$	2σ	$^{208}Pb/^{206}Pb$	2σ
Core C3										
0–1.1	18.285	0.004	15.617	0.005	38.28	0.02	1.1709	0.0001	2.0933	0.0004
1.1–2.2	18.343	0.003	15.655	0.004	38.44	0.01	1.1717	0.0001	2.0956	0.0003
2.2–3.3	18.337	0.011	15.656	0.011	38.45	0.03	1.1712	0.0002	2.0973	0.0004
3.3–4.4	18.416	0.005	15.668	0.006	38.60	0.02	1.1755	0.0001	2.0957	0.0005
4.4–5.5	18.443	0.009	15.729	0.060	38.75	0.02	1.1725	0.0001	2.1013	0.0005
‡4.4–5.5	18.394	0.014	15.668	0.007	38.60	0.02	1.1739	0.0001	2.0984	0.0006
5.5–6.6	18.429	0.007	15.669	0.007	38.57	0.02	1.1761	0.0001	2.0928	0.0004
6.6–7.7	18.468	0.004	15.681	0.004	38.70	0.01	1.1777	0.0001	2.0956	0.0004
7.7–8.8	18.487	0.015	15.703	0.035	38.71	0.04	1.1774	0.0002	2.0939	0.0004
8.8–9.9	18.456	0.005	15.643	0.005	38.56	0.01	1.1799	0.0001	2.0890	0.0003
9.9–11	18.519	0.008	15.658	0.008	38.66	0.02	1.1826	0.0001	2.0877	0.0003
13–14	18.502	0.015	15.591	0.013	38.46	0.03	1.1867	0.0002	2.0788	0.0003
‡13–14	18.602	0.004	15.679	0.004	38.65	0.01	1.1864	0.0001	2.0776	0.0004
14–15	18.555	0.004	15.617	0.004	38.56	0.01	1.1881	0.0001	2.0780	0.0004
18–19	18.686	0.012	15.709	0.011	38.81	0.03	1.1895	0.0002	2.0766	0.0004
21–22	18.650	0.003	15.665	0.003	38.76	0.01	1.1906	0.0002	2.0782	0.0003
27–28	18.661	0.005	15.667	0.005	38.80	0.02	1.1909	0.0001	2.0790	0.0003
33–34	18.706	0.006	15.672	0.006	38.77	0.02	1.1936	0.0001	2.0725	0.0003
41–42	18.757	0.006	15.662	0.006	38.70	0.02	1.1976	0.0001	2.0633	0.0003
47–49	18.648	0.009	15.648	0.009	38.58	0.02	1.1941	0.0002	2.0683	0.0004
53–54	18.697	0.015	15.638	0.014	38.70	0.04	1.1956	0.0002	2.0699	0.0004
62–63	18.744	0.008	15.663	0.008	38.74	0.02	1.1966	0.0001	2.0667	0.0003
73–74	18.764	0.004	15.668	0.004	38.78	0.01	1.1976	0.0001	2.0669	0.0003
Core C4										
0–1	18.296	0.006	15.647	0.006	38.40	0.02	1.1692	0.0001	2.0985	0.0003
1–2	18.295	0.013	15.639	0.011	38.34	0.03	1.1695	0.0001	2.0962	0.0005
2–4	18.341	0.002	15.618	0.003	38.37	0.01	1.1743	0.0001	2.0916	0.0003
4–5	18.445	0.013	15.662	0.012	38.58	0.03	1.1776	0.0003	2.0916	0.0006
5–7	18.487	0.005	15.680	0.006	38.67	0.02	1.1791	0.0002	2.0915	0.0005
7–8.5	18.493	0.003	15.675	0.004	38.66	0.01	1.1797	0.0001	2.0903	0.0003
8.5–10	18.493	0.010	15.668	0.009	38.61	0.02	1.1803	0.0001	2.0879	0.0004
10–11.5	18.462	0.007	15.628	0.007	38.53	0.02	1.1813	0.0002	2.0870	0.0003
11.5–12.5	18.471	0.003	15.645	0.004	38.55	0.01	1.1806	0.0001	2.0872	0.0003
12.5–14	18.492	0.003	15.638	0.004	38.56	0.01	1.1825	0.0001	2.0855	0.0003
16–17	18.586	0.003	15.674	0.003	38.73	0.01	1.1858	0.0001	2.0840	0.0003
19–20	18.567	0.036	15.613	0.031	38.58	0.08	1.1892	0.0002	2.0776	0.0007
‡19–20	18.624	0.004	15.651	0.004	38.59	0.01	1.1900	0.0001	2.0722	0.0002
22–23	18.647	0.003	15.664	0.003	38.71	0.01	1.1904	0.0001	2.0758	0.0003
29–30	18.685	0.004	15.652	0.005	38.70	0.01	1.1938	0.0001	2.0709	0.0003
‡29–30	18.689	0.013	15.653	0.012	38.64	0.03	1.1939	0.0002	2.0680	0.0004
35–36	18.715	0.008	15.684	0.007	38.82	0.02	1.1932	0.0001	2.0744	0.0004
‡35–36	18.695	0.003	15.660	0.003	38.69	0.01	1.1938	0.0001	2.0695	0.0003
40–41	18.726	0.007	15.691	0.008	38.80	0.02	1.1936	0.0002	2.0720	0.0004
48–49	18.676	0.005	15.650	0.005	38.65	0.02	1.1934	0.0001	2.0694	0.0004
60–61	18.682	0.003	15.670	0.004	38.72	0.01	1.1921	0.0001	2.0725	0.0003
71–72	18.646	0.005	15.632	0.005	38.59	0.02	1.1928	0.0001	2.0698	0.0003

domestic effluents, smelting operations, mining repositories, and burning of fossil fuel. The aim of this study is the reconstruction of the long-term history of Pb pollution in this environment, using its concentrations and isotopic compositions in the sediments. This work supplements previously published studies dealing with short-term variations of heavy metals entering the basin (fluxes and origins) via surficial waters (Monna et al., 1995; Petelet et al., 1997), and a study of contouring Pb concentrations in the bed sediments of the basin (Péna, 1989). An extraction procedure was designed to release Pb bound in different ways to the sediment. The resulting fractional Pb release provided information about the origin of the Pb and the identifi-

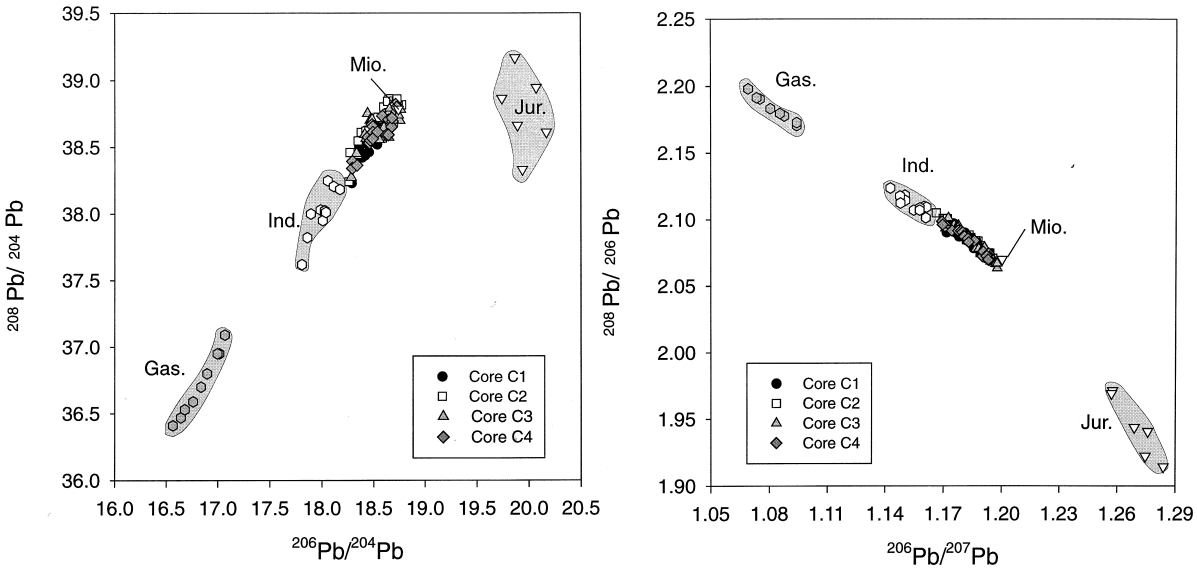

Fig. 2. $^{208}Pb/^{204}Pb$ vs $^{206}Pb/^{204}Pb$ and $^{208}Pb/^{206}Pb$ vs $^{206}Pb/^{207}Pb$ ratios of the untreated bulk sediments from cores C1–4. The Pb isotopic compositions of the potential sources are also reported: open triangles for the local Jurassic and Miocene rocks (=Jur. and Mio. areas) after leaching or total dissolution (Petelet et al., 1997), open hexagons for the present-day industrial source consisting of ashes from an incinerator of the city of Sète and a domestic-water treatment plant (=Ind. areas), and closed hexagons for the present-day leaded gasoline (=Gas areas) signature (Monna et al., 1995, 1997b).

cation of the mineral phases with which the anthropogenic Pb is primarily associated.

2. Description of the site area

The Thau lake is located approximately 20 km to the south of Montpellier in southern France (Fig. 1). It covers a surface area of 70 km^2, with a depth averaging 5 m and reaching locally 11 m; it has a volume of 265 Mm^3. Divided into three parts (the Crique de l'Angle, the Etang des Eaux Blanches close to Sète, and the Grand Etang), it is separated from the Mediterranean Sea by a narrow shore bar allowing limited exchanges with the open sea only through three navigation channels. In its northern part, several rivers feed the lake, but most of them are dry, except during heavy rainfall. The Vène is the major river feeding the lake at the Crique de l'Angle.

Many potential sources of pollution exist around the lake. Domestic and industrial waste waters are released into the basin either directly or after treatment. A road network with a highway, heavily used by a daily average of 37,000 cars, crosses the area. In addition, many industrial plants are located around the city of Sète, which is the main city of the basin with its 41,000 inhabitants.

3. Methods and results

Four cores (between 0.4 and 1 m in length) were sampled with a "McKareth" corer. To identify each type of Pb contribution, the cores were located relative to the potential Pb sources. Core C1 was drilled in the centre of the Etang des Eaux Blanches close to the city of Sète, to target the industrial and urban contributions. Cores C2 and C3 were sampled in the Crique de l'Angle close to the mouth of the Vène river. Core C4 was sampled in the centre of the Grand Etang.

Details of the coring technique, and sample collection and preparation are available in Monna et al. (1996, 1997a). Dating of the sediment deposits was carried out using the ^{210}Pb method. In this dating method, activity of the ^{210}Po isotope assumed to be in secular equilibrium with the ^{210}Pb, was measured by Photon/Electron-Rejecting Alpha Liquid Scintillation (Monna et al., 1996). In each core, one horizon was clearly identified by its strong terrigenous signature and by X-ray. This unit was attributed to the exceptional flooding that is known to have devastated the whole region in September 1875. The depths of the unit in the cores agree well with those expected from calculated sedimentation rates. This identity enabled the extension of ^{210}Pb-based chronology over the last 150 years (Monna et al., 1997a).

Two chemical procedures were applied to the collected sediments. One consisted of total digestions of

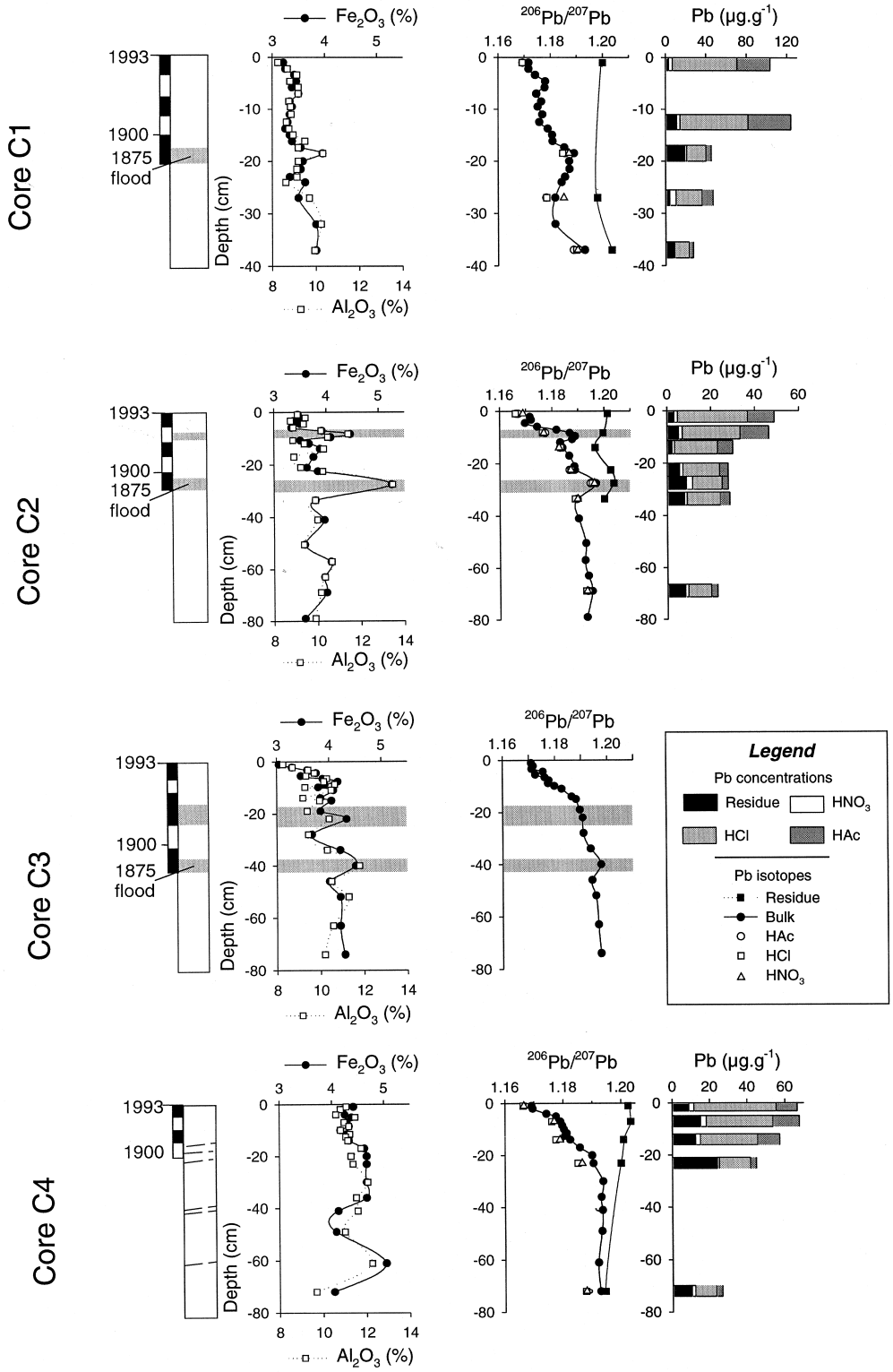

Fig. 3. Cores C1–C4. Fe_2O_3, Al_2O_3 (data from Monna et al., 1997a), $^{206}Pb/^{207}Pb$ ratio and Pb profiles relative to depth. The $^{206}Pb/^{207}Pb$ ratios were determined on the bulk fraction, <60 µm, on the leachates by HAc, HCl and HNO_3, and on the residues.

about 50 mg of the total <60 μm sediment fraction in a mixture of 2 ml of ultrapure concentrated HNO_3, HCl, and HF. The second procedure consisted of a sequential digestion of 17 samples for which approximately 400 mg of sediments were successively leached with 30 ml of 1N HAc, 1N HCl, and 1N HNO_3. The different leachates were analysed independently and the final residues were digested in HF afterwards, as above. For each aliquot, Pb was purified on micro-columns of AG1X4 resin. The isotopic compositions of Pb were measured on a VG SECTOR thermo-ionisation mass spectrometer (TIMS) using static multi-collection (Monna et al., 1995). Repetitive measurements showed that the $^{206}Pb/^{207}Pb$ ratios were by far the most reproducible with a level of significance in the fourth decimal, while the variations of the $^{206}Pb/^{204}Pb$ ratios were significant in the second decimal. To control the efficiency and the effects of the leachings, the contents of Ca, Fe, Mg, Si and Al were systematically determined by ICP-AES, whereas those of Pb and Th were measured on an ICP–MS following a procedure similar to that described by Roberts and Ruiz (1989). Replicate analyses of samples and standards indicated an accuracy within $\pm 5\%$.

The $^{206}Pb/^{207}Pb$ ratios of the bulk sediments are constant in the deepest part of the cores (Table 1, Figs. 2, 3). They decrease more or less regularly upwards, to reach values ranging between 1.166 and 1.171 at the top of the cores. Shifts of the ratio to higher values were also found, twice in the core C2 (at depths of ~8–10 cm and ~25–27 cm), once in the core C3 (at ~40–42 cm) and once in the core C1 (at ~17–20 cm), while the strongly intercorrelated Fe_2O_3 and the Al_2O_3 contents showed significant enrichments at the same depths. These levels were clearly identified on X-ray radiographs in the cores C2 and C3 by an opaque aspect contrasting with the normal sedimentary sequence (grey boxes in Fig. 3). They consist of very fine and homogeneous material totally devoid of marine organisms. Core C4 yields a regular decrease of the $^{206}Pb/^{207}Pb$ ratio from base to top, with a slight inflection between 7 and 12 cm which could have been induced by a significant increase of the sedimentation rate (Monna et al., 1997a).

Among the different leachates, the HAc one yields the highest Ca (about 90–95% of the total Ca) and Mg contents, suggesting dissolution of carbonate mineral phases. The HCl leachates contain more Si and Al and yield the highest Fe concentrations, implying that Fe-oxyhydroxides were leached at this step of the experiment. The HNO_3 leachates yield the highest Si contents, but less Al, Mg, Ca and Fe, suggesting oxidation of the organic matter. The Pb isotope compositions of the HAc, HCl and HNO_3 leachates are very similar (Table 2, Fig. 3). They are always less radiogenic than those of the corresponding untreated bulk

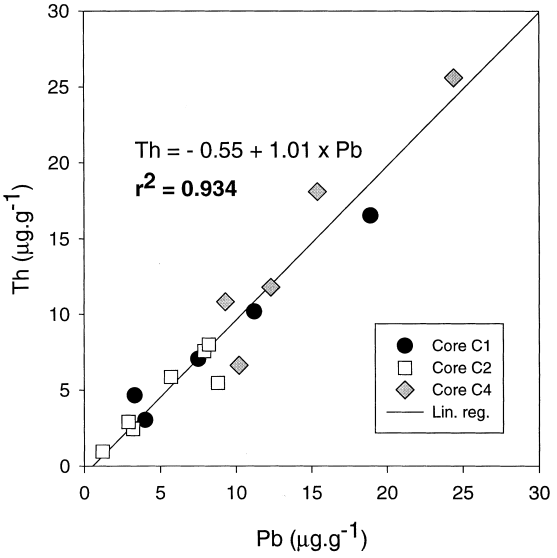

Fig. 4. Pb vs Th in the residual fractions.

sediment. Consequently, the residues are systematically more radiogenic than the bulk material. The total Pb contents measured at the bottom are similar in all of the cores (23–27 μg g^{-1}); they increase toward the surface to reach varied values at the top: 103, 49 and 67 μg g^{-1} for cores C1, C2 and C4, respectively.

Between 80 and 99% of Th, and almost all Zr (not shown here) are hosted by the silici-clastic residues. At the base, approximately 40–60% of Pb belongs to the leachates and residues, respectively, whereas in the uppermost sediment almost all of the Pb was released by the HAc and HCl reagents. The HNO_3 leaching always removed insignificant amounts of Pb compared to the total Pb contents.

4. Discussion

Plots of the $^{208}Pb/^{204}Pb$ and the $^{208}Pb/^{206}Pb$ ratios against the $^{206}Pb/^{204}Pb$ and $^{206}Pb/^{207}Pb$ ratios of the untreated bulk sediments from four cores (Fig. 2) suggest a two- (or more) component mixing of lithogenic Pb with anthropogenic inputs increasing towards the top of the cores. These latter inputs are characterised by distinctly lower radiogenic isotopic signatures (Fig. 3).

4.1. Lithogenic sources of Pb

The lithogenic Pb component in the lake sediments derives basically from Jurassic limestones, Cretaceous sandstones and Miocene claystones constituting the watershed. However, a systematic and representative

Table 2
Pb isotopic compositions and Pb–Th contents. expressed in μg g^{-1}. after sequential leaching experiments (see text for details) (–, not determined)

	$^{206}Pb/^{204}Pb$	2σ	$^{207}Pb/^{204}Pb$	2σ	$^{208}Pb/^{204}Pb$	2σ	$^{206}Pb/^{207}Pb$	2σ	$^{208}Pb/^{206}Pb$	2σ	Pb ± 5%	Th ± 5%
C1 0–1												
HAc	18.278	0.008	15.631	0.008	38.31	0.02	1.1694	0.0001	2.0955	0.0004	32.7	0.09
HCl	18.281	0.004	15.634	0.004	38.37	0.01	1.1693	0.0001	2.0966	0.0004	63.8	0.20
HNO_3	–	–	–	–	–	–	–	–	–	–	3.7	0.19
Residue	18.780	0.036	15.655	0.031	38.90	0.08	1.2000	0.0003	2.0706	0.0003	3.2	4.64
Bulk	18.290	0.006	15.612	0.007	38.23	0.02	1.1716	0.0001	2.0902	0.0003	103.4	5.12
C1 11–12.5												
HAc	–	–	–	–	–	–	–	–	–	–	42.1	0.14
HCl	–	–	–	–	–	–	–	–	–	–	67.0	0.11
HNO_3	–	–	–	–	–	–	–	–	–	–	3.6	0.09
Residue	–	–	–	–	–	–	–	–	–	–	11.0	10.2
Bulk	18.386	0.012	15.638	0.011	38.53	0.03	1.1757	0.0001	2.0956	0.0005	123.9	10.5
C1 17.4–18.5												
HAc	18.570	0.006	15.662	0.006	38.67	0.02	1.1856	0.0001	2.0812	0.0003	5.0	0.06
HCl	18.602	0.012	15.703	0.011	38.77	0.03	1.1847	0.0001	2.0841	0.0004	19.1	0.08
HNO_3	18.584	0.006	15.654	0.005	38.61	0.02	1.1872	0.0001	2.0775	0.0003	1.8	0.05
Residue											19.2	16.5
Bulk	18.606	0.014	15.649	0.012	38.63	0.03	1.1890	0.0001	2.0762	0.0004	45.2	16.7
C1 26–27												
HAc	18.428	0.006	15.639	0.006	38.49	0.02	1.1784	0.0001	2.0883	0.0004	10.7	0.09
HCl	18.470	0.009	15.671	0.008	38.64	0.02	1.1786	0.0001	2.0921	0.0004	25.8	0.10
HNO_3	18.569	0.009	15.667	0.009	38.62	0.02	1.1851	0.0001	2.0798	0.0003	6.3	0.60
Residue	18.768	0.003	15.664	0.004	38.81	0.01	1.1982	0.0001	2.0681	0.0003	4.0	3.2
Bulk	18.484	0.006	15.641	0.006	38.60	0.02	1.1818	0.0001	2.0883	0.0003	46.8	3.8
C1 36–37												
HAc	18.620	0.006	15.662	0.006	38.67	0.02	1.1888	0.0001	2.0766	0.0003	4.1	0.10
HCl	18.628	0.004	15.654	0.004	38.65	0.01	1.1899	0.0001	2.0746	0.0003	14.3	0.15
HNO_3	18.663	0.007	15.678	0.006	38.73	0.03	1.1904	0.0001	2.0751	0.0003	1.3	0.06
Residue	–	–	–	–	–	–	1.2035	0.0020	2.0597	0.0045	7.6	7.0
Bulk	18.693	0.003	15.667	0.004	38.70	0.01	1.1931	0.0001	2.0705	0.0003	27.2	7.3
C2 0–1 cm												
HAc	18.235	0.004	15.625	0.004	38.26	0.01	1.1671	0.0001	2.0981	0.0004	12.0	0.07
HCl	18.265	0.006	15.663	0.007	38.40	0.02	1.1660	0.0002	2.1026	0.0006	32.1	0.09
HNO_3	18.287	0.006	15.644	0.006	38.34	0.02	1.1689	0.0001	2.0965	0.0003	1.6	0.03
Residue	18.827	0.007	15.673	0.007	38.92	0.02	1.2013	0.0001	2.0670	0.0003	3.2	2.45
Bulk	18.272	0.003	15.666	0.003	38.46	0.01	1.1663	0.0001	2.1050	0.0003	49.0	2.65
C2 7.2–8.4 cm												
HAc	18.417	0.004	15.642	0.004	38.47	0.01	1.1774	0.0001	2.0887	0.0003	13.1	0.10
HCl	18.441	0.004	15.676	0.004	38.62	0.01	1.1764	0.0001	2.0941	0.0003	26.4	0.08

HNO_3	18.445	0.005	15.672	0.005	38.60	0.01	1.1769	0.0001	2.0928	0.0003	1.7	0.04
Residue	18.816	0.011	15.682	0.010	38.91	0.03	1.1996	0.0001	2.0685	0.0003	1.2	0.96
Bulk	18.589	0.004	15.663	0.004	38.72	0.01	1.1868	0.0001	2.0827	0.0003	46.5	1.2
C2 13–14 cm												
HAc	18.526	0.005	15.658	0.005	38.60	0.02	1.1831	0.0001	2.0834	0.0003	7.0	0.08
HCl	18.564	0.004	15.687	0.004	38.76	0.01	1.1834	0.0001	2.0879	0.0003	19.6	0.16
HNO_3	18.489	0.009	15.631	0.005	38.51	0.02	1.1828	0.0001	2.0832	0.0003	1.2	0.05
Residue	18.738	0.005	15.660	0.005	38.80	0.01	1.1965	0.0001	2.0707	0.0003	2.9	2.9
Bulk	18.599	0.006	15.707	0.006	38.81	0.02	1.1840	0.0001	2.0864	0.0004	30.0	3.2
C2 21–22.5 cm												
HAc	18.573	0.006	15.650	0.005	38.59	0.02	1.1867	0.0001	2.0775	0.0005	3.9	0.06
HCl	18.609	0.006	15.675	0.006	38.67	0.02	1.1872	0.0001	2.0779	0.0003	16.4	0.11
HNO_3	18.585	0.007	15.655	0.006	38.65	0.02	1.1872	0.0001	2.0795	0.0003	1.7	0.05
Residue	18.868	0.026	15.696	0.022	38.95	0.05	1.2025	0.0002	2.0637	0.0004	5.7	5.9
Bulk	18.630	0.006	15.671	0.007	38.76	0.02	1.1887	0.0001	2.0803	0.0003	27.9	6.1
C2 26.5–27.5 cm												
HAc	18.739	0.008	15.684	0.008	38.78	0.02	1.1947	0.0001	2.0693	0.0005	2.8	0.09
HCl	18.755	0.006	15.689	0.005	38.77	0.02	1.1954	0.0001	2.0667	0.0003	13.5	0.07
HNO_3	18.747	0.006	15.672	0.006	38.69	0.02	1.1962	0.0001	2.0637	0.0003	2.8	0.06
Residue	18.877	0.006	15.683	0.005	38.84	0.02	1.2037	0.0001	2.0577	0.0003	8.8	5.5
Bulk	18.776	0.005	15.687	0.005	38.82	0.02	1.1969	0.0001	2.0673	0.0003	27.9	5.6
C2 32.5–33.5 cm												
HAc	18.612	0.006	15.646	0.006	38.58	0.02	1.1895	0.0001	2.0729	0.0003	4.3	0.07
HCl	18.631	0.005	15.673	0.005	38.69	0.01	1.1889	0.0001	2.0764	0.0003	15.2	0.16
HNO_3	18.627	0.004	15.656	0.004	38.63	0.01	1.1898	0.0001	2.0735	0.0003	1.2	0.05
Residue	18.813	0.003	15.668	0.003	38.84	0.01	1.2006	0.0001	2.0647	0.0003	7.9	7.6
Bulk	18.654	0.003	15.679	0.004	38.72	0.01	1.1897	0.0001	2.0760	0.0003	28.5	7.8
C2 68–69 cm												
HAc	18.695	0.012	15.663	0.011	38.69	0.03	1.1936	0.0001	2.0698	0.0003	2.8	0.09
HCl	18.717	0.004	15.689	0.004	38.79	0.01	1.1930	0.0001	2.0721	0.0002	10.4	0.13
HNO_3	18.691	0.004	15.664	0.005	38.68	0.01	1.1933	0.0001	2.0694	0.0003	1.4	0.05
Residue	–	–	–	–	–	–	–	–	–	–	8.2	8.0
Bulk	18.754	0.006	15.708	0.006	38.89	0.02	1.1954	0.0001	2.0713	0.0004	22.9	8.2
C4 0–1												
HAc	18.252	0.003	15.651	0.004	38.34	0.01	1.1662	0.0001	2.1006	0.0003	11.2	0.07
HCl	18.266	0.005	15.653	0.003	38.39	0.01	1.1669	0.0001	2.1017	0.0003	43.7	0.15
HNO_3	18.249	0.003	15.647	0.005	38.42	0.01	1.1663	0.0001	2.1053	0.0004	2.6	0.11
Residue	–	–	–	–	–	–	1.2025	0.0005	2.0570	0.0007	9.0	10.8
Bulk	18.296	0.006	15.647	0.006	38.40	0.02	1.1692	0.0001	2.0985	0.0003	66.5	11.1
C4 5–7												
HAc	18.424	0.003	15.647	0.003	38.53	0.01	1.1775	0.0001	2.0915	0.0003	13.9	0.11
HCl	18.436	0.004	15.674	0.005	38.63	0.01	1.1762	0.0001	2.0951	0.0003	35.5	0.13
HNO_3	18.413	0.009	15.642	0.008	38.48	0.02	1.1770	0.0001	2.0904	0.0003	3.1	0.13
Residue	–	–	–	–	–	–	1.2034	0.0005	2.0587	0.0008	15.2	18.8

(continued on next page)

Table 2 (*continued*)

	$^{206}Pb/^{204}Pb$	2σ	$^{207}Pb/^{204}Pb$	2σ	$^{208}Pb/^{204}Pb$	2σ	$^{206}Pb/^{207}Pb$	2σ	$^{208}Pb/^{206}Pb$	2σ	Pb ± 5%	Th ± 5%
Bulk	18.487	0.005	15.680	0.006	38.67	0.02	1.1791	0.0001	2.0915	0.0005	67.8	18.5
C4 13–14												
HAc	18.453	0.003	15.642	0.003	38.51	0.01	1.1796	0.0001	2.0871	0.0001	11.7	0.09
HCl	18.501	0.003	15.711	0.003	38.76	0.01	1.1776	0.0001	2.0949	0.0004	30.5	0.10
HNO_3	18.459	0.007	15.656	0.006	38.56	0.02	1.1789	0.0001	2.0895	0.0004	2.7	0.10
Residue	18.815	0.008	15.668	0.007	38.82	0.02	1.2009	0.0001	2.0633	0.0003	12.4	11.8
Bulk	18.492	0.003	15.638	0.004	38.56	0.01	1.1825	0.0001	2.0855	0.0003	57.2	12.1
C4 22–23												
HAc	18.586	0.006	15.665	0.005	38.61	0.02	1.1865	0.0001	2.0775	0.0003	3.2	0.10
HCl	18.587	0.003	15.683	0.005	38.73	0.01	1.1851	0.0001	2.0838	0.0003	16.5	0.08
HNO_3	18.571	0.006	15.651	0.007	38.57	0.02	1.1866	0.0001	2.0777	0.0003	1.15	0.06
Residue	18.814	0.028	15.676	0.023	38.89	0.06	1.2002	0.0003	2.0671	0.0003	24.0	25.6
Bulk	18.647	0.003	15.664	0.003	38.71	0.01	1.1904	0.0001	2.0757	0.0003	44.9	25.8
C4 71–72												
HAc	18.602	0.008	15.642	0.007	38.60	0.02	1.1892	0.0001	2.0747	0.0003	3.3	0.13
HCl	18.651	0.005	15.703	0.005	38.75	0.01	1.1878	0.0001	2.0775	0.0003	11.2	0.14
HNO_3	18.618	0.005	15.671	0.005	38.64	0.02	1.1880	0.0001	2.0753	0.0003	1.9	0.06
Residue	18.752	0.017	15.701	0.015	38.87	0.04	1.1946	0.0002	2.0724	0.0007	10.2	6.6
Bulk	18.646	0.005	15.632	0.005	38.60	0.02	1.1928	0.0001	2.0697	0.0003	26.6	6.9

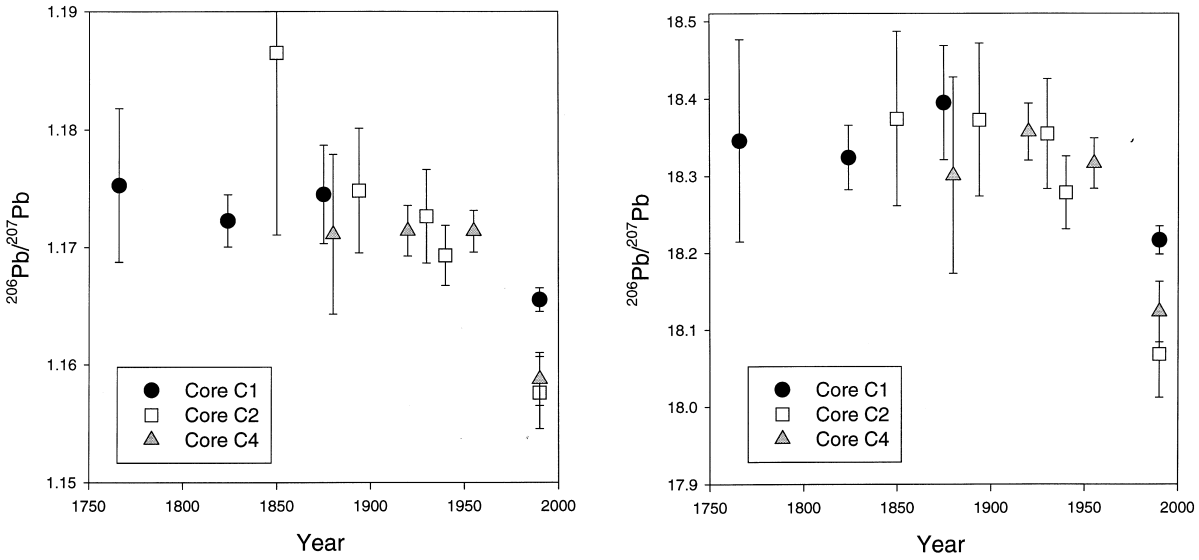

Fig. 5. Pb-isotopic evolution of the anthropogenic component during the last 200 years.

sampling to define isotopically the lithogenic Pb is not straightforward, as its signature may vary in the whole sedimentary sequence.

Partial rock weathering releases more radiogenic Pb from metamict U- and Th-rich minerals (Erel et al., 1990; 1991; Keinonen, 1992; Puchelt et al., 1993), implying that a detrital part of the sediment would have lower radiogenic signatures than any Pb transported in solution (primarily leached from precursor rocks), and trapped afterwards in authigenic phases. In fact, the leachates are systematically less radiogenic than the residues, even in the deepest horizons deposited more than 200 years ago. Consequently, the less radiogenic (=anthropogenic) component may be identified as early as that time, and even further back in time as seen in an ombrotrophic bog in the Jura (Shotyk et al., 1996). Although the specific input of anthropogenic Pb is difficult to evaluate here in the oldest samples because of the large amounts of lithogenic material, it is systematically visible. However, the lithogenic end-member may be assessed from the signature of the residues with a $^{206}Pb/^{207}Pb$ ratio of ca. 1.20. This assumption is supported by the fact that Th and Zr, which are typically terrigenous elements, are strongly correlated with the Pb contents in the residual phases (cf Fig. 4). As outlined by their positions in the Pb diagram, the Jurassic limestones should not play a major role as Pb suppliers (Fig. 2), while the Miocene clays seem to be better candidates.

4.2. Anthropogenic sources of Pb

In a sedimentary sequence, simultaneous variations in Pb contents and isotopic compositions may be attributed to anthropogenic influences (Croudace and Cundy, 1995; Graney et al., 1995; Hamelin et al., 1990; Hamilton and Clifton, 1979; Hirao et al., 1986; Öhlander et al., 1993; Petit, 1974; Petit et al., 1984; Ritson et al., 1994; Shirahata et al., 1980). It may be safely assumed that the isotopic signature of anthropogenic Pb is different from local rock-derived Pb. This is often the case in France, at least since the mid 1960s, where two main anthropogenic sources could be isotopically distinguished for Pb (Elbaz-Poulichet et al., 1984; Monna et al., 1995, 1997b). The less radiogenic is the Pb added as an anti-knock compound to gasoline ($^{206}Pb/^{207}Pb$ ratio between 1.069 and 1.094, n = 9), which mainly derives from the Precambrian ore deposits of Australia and Canada. The Pb of industrial origin is apparently rather homogeneous and more radiogenic: from 1992 to 1995, isotopic analyses of ashes coming from an urban incinerator in Sète city provided $^{206}Pb/^{207}Pb$ ratios of 1.142–1.154 (n = 4), and those of domestic waste waters entering the Thau lake gave $^{206}Pb/^{207}Pb$ ratios of 1.146–1.162 (n = 14). These values certainly represent reliable information of the current situation, but the past isotopic evolution is much less constrained; only a few data having been reported (Chow et al., 1975; Elbaz-Poulichet et al., 1984, 1986; Flament, 1985; Grousset et al., 1994, 1995). They suggest that the Pb signatures of gasoline and industrial sources remained more or less constant only over the last 20 years. Extension of such a database to the older past is probably inadequate.

The Pb isotopic composition of the anthropogenic component [$(^{206}Pb/^{207}Pb)_{Anthr.}$] in the different lea-

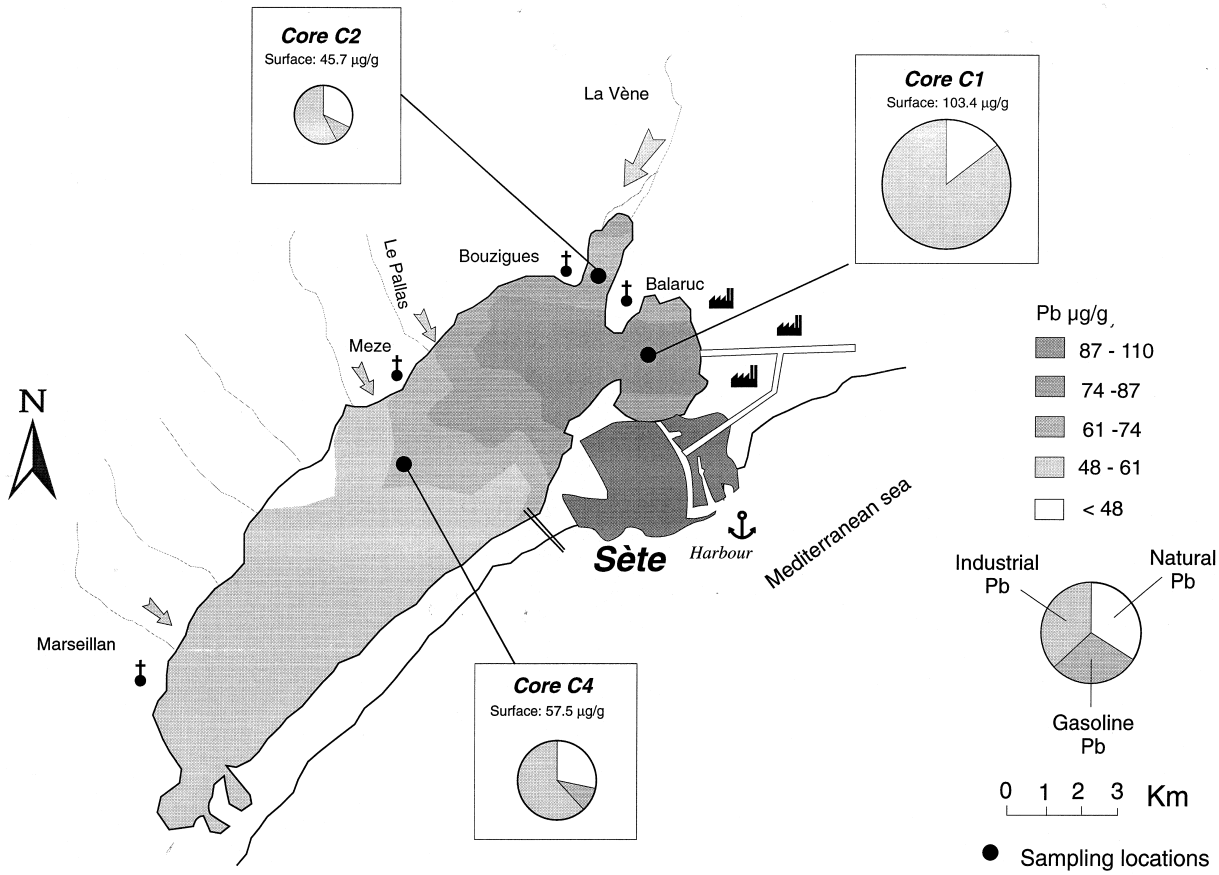

Fig. 6. Map of Pb concentrations in the bed sediments of the Thau lake (Péna, 1989). For comparison, the concentrations measured at the top of the cores in this study, are reported with the proportions of their three potential origins being natural, industrial/domestic and leaded gasoline.

chates can be mathematically expressed as:

$$(^{206}Pb/^{207}Pb)_{Anthr.} = [(^{206}Pb/^{207}Pb)_{TL} \cdot C_{TL} - (^{206}Pb/^{207}Pb)_{BC} \cdot C_{BC}]/(C_{TL} - C_{BC})$$

where $(^{206}Pb/^{207}Pb)_{TL}$ and C_{TL} are the isotopic compositions and concentrations of the total leached Pb, while $(^{206}Pb/^{207}Pb)_{BC}$ and C_{BC} correspond to the total amount of Pb supposedly having a lithogenic origin with a $(^{206}Pb/^{207}Pb)_{BC}$ ratio of 1.200 ± 0.003 and a C_{BC} concentration of 10 ± 3 µg g^{-1} (Table 2). These values derive from the deepest samples of the cores, assuming that they are representative of the past values. It is actually likely that various anthropogenic activities in and around the basin with agriculture modifying the erosion/weathering processes since 1800, maintenance of the channels connecting the lake with the sea, and drainage diversions due to the construction of the highways, modified the detrital inputs into the lake. The basin also received sudden and massive amounts of terrigenous material during major flooding events (Monna et al., 1997a). The shifts of the Pb isotopic ratios in these units towards the lithogenic values, as well as the increase of the Al and Fe contents, corroborate the previous findings.

If these flood deposits are discarded, the history and the origin of the Pb pollution can be fairly assessed. The Etang des Eaux Blanches has always been the most polluted area of the basin, probably because of the proximity of the city of Sète. With industrialisation, the pollution considerably increased at the beginning of the 20th century. Since recent adoption of controls, the pollution in the area has decreased, but not enough data are presently available to determine precisely when the turning point really occurred. The other areas of the lake follow roughly the same evolution, but to a lesser extent.

The isotopic signatures of the anthropogenic com-

ponent remained steady during the 1800–1950 period with $^{206}Pb/^{204}Pb$ ratios of 18.25–18.40, and $^{206}Pb/^{207}Pb$ ratios of 1.170–1.175 (Fig. 5). The ratios began to decrease since 1950. Similar 'excess' Pb ratios were measured in the UK for the 1865–1890 period (Bacon et al., 1996), and in Scottish lakes until the introduction of Pb additives to gasoline (Farmer et al., 1993). As in the UK before the introduction of gasoline Pb, the anthropogenic Pb in the sediments of Thau lake should mainly relate to domestic Pb ore bodies and coal burning emissions. The continued decrease to lower radiogenic signatures, which indicates increasing use of imported Pb, occurred later in France (post 1950s) than in the UK (during the 1940s).

In fact, the only noticeable differences among the three cores is observed at the surface of the sediment, where the $(^{206}Pb/^{207}Pb)_{Anthr.}$ ratios of cores C2 (1.155 $\pm$ 0.001) and C4 (1.155 $\pm$ 0.004) are slightly lower than that of core C1 (1.164 $\pm$ 0.002). The signature at the top of core C1 likely reflects the overall inputs of the nearby city of Sète. For the other cores, another less radiogenic component has to be considered. It could be the domestic waste waters of the neighbouring villages (for which the $^{206}Pb/^{207}Pb$ ratio was identified to be as low as 1.147), or leaded gasoline. As a matter of fact, it has been locally demonstrated that a significant input of gasoline-derived Pb could occur during rainfall (Monna et al., 1995; Petelet et al., 1997), but it can be calculated that the leaded gasoline does not contribute more than 10% of the total Pb contained in the most recent sediments. As a consequence, the anthropogenic Pb mainly comes from other human activities, such as domestic or industrial inputs.

The present results agree well with the distribution of Pb in the superficial sediments of the lake (Fig. 6, Péna, 1989). This map shows a significant concentration of heavy metals centred on the city of Sète, suggesting that it influences greatly the supply to the lake sediments. From the city towards the opposite end of the lake, the Pb contamination becomes lower, and consequently the relative proportion of Pb coming from gasoline may increase.

The Pb concentrations of the three types of leachates are significantly different: those of the HCl leachates are systematically the highest and those of the HNO_3 leachates are systematically the lowest. This means that the soluble Pb is preferentially incorporated by oxyhydroxide phases, and that only a very small amount is strongly associated with organic matter. Adsorption of Pb onto organic material, which is considered usually to play an important role in sediments, has a minor effect on the studied cores. This is shown by significantly low contents of Pb in the HNO_3 leachates, which are basically representative of the organic matter. The fact that the HCl leachates consistently appear to have higher $^{207}Pb/^{204}Pb$ ratios (and to some extent higher $^{208}Pb/^{204}Pb$ ratios) than the HAc and the HNO_3 leachates, suggest that the contaminant compound soluble in HCl is slightly different than that removed by HAc.

5. Conclusions

Before the 19th century, the Pb entering the Thau basin had mostly a lithogenic origin with $^{206}Pb/^{207}Pb$ ratios of less than 1.20. From the beginning of the 19th century, the supply of anthropogenic Pb increased in the sediments of the Etang des Eaux Blanches, which continued to receive increased inputs from the city of Sète. This area has probably always been the most polluted part of the lake with a considerable increase of Pb contents as early as the 20th century. The central part of the basin and the Crique de l'Angle have approximately the same history, but with less Pb pollution since the anthropogenic contribution from the city of Sète was diluted by terrigenous inputs. Today, only the Pb coming from the industrial/domestic input of Sète can be distinguished in the Etang des Eaux Blanches. Even if a small contribution of Pb coming from the automotive source is, to some extent, also detectable in the two other sites, it seems that the Pb of industrial/domestic origin is the major contributor to the whole basin.

This study also shows that the anthropogenic Pb component was fairly stable from about 1800 until the 1950s with $^{206}Pb/^{204}Pb$ ratios of 18.25–18.40 and $^{206}Pb/^{207}Pb$ ratios of 1.170–1.175. Afterwards, the supply of anthropogenic Pb decreased as the $^{206}Pb/^{204}Pb$ ratio decreased to 18.10–18.25 and the $^{206}Pb/^{207}Pb$ ratio to 1.155–1.165, presumably because of an increased use of a remotely-derived low-radiogenic Pb. In addition, most of the anthropogenic Pb is associated with oxides and hydroxides, minor amounts being trapped in authigenic carbonates, or simply adsorbed on mineral particles and only a few seem to be linked to organic matter.

Acknowledgements

Our sincere thanks are due to Dr P. Fritz (University of Leipzig, Germany) and to an anonymous reviewer for their careful review that helped to improve the script, as well as to Drs J.D. Kramers (University of Bern, Switzerland) and J.N. Connelly (University of Texas at Austin, USA) for thorough comments on an earlier draft. We wish also to thank Dr S. Chaudhuri (Kansas State University, USA) for having improved the English presentation. A. Allegret, K. Ben Barak, A.-S. Escudié, R. Kretz and O. Michel are thanked for help during sampling, as well as M. Taïeb, D. William-

son (University of Luminy-Marseille, France) for kindly lending the "Mackereth" corer, and J. Samuel and R. Rouault (Centre de Géochimie de la Surface, CNRS–ULP, Strasbourg, France) for assistance in the ICP–AES and ICP–MS determinations. T.T. acknowledges the financial help of the Deutsche Forschungsgemeinschaft (Project Kr-590/34).

References

Bacon, J.R., Jones, K.C., McGrath, S.P., Johnson, A.E., 1996. Isotopic character of lead deposited from the atmosphere at a grassland site in the United Kingdom since 1860. Environ. Sci. Technol. 30, 2511–2518.

Chow, T.J., Snyder, C.B., Earl, J.L., 1975. Isotope ratios of lead as pollutant source indicator. In: Proceedings of the United Nations FAO and International Atomic Energy Association Symposium, Vienna, Austria (IAEA-SM-191/4). pp. 95–108.

Croudace, I.W., Cundy, A.B., 1995. Heavy metal and hydrocarbon pollution in recent sediments from Southampton water, southern England: a geochemical and isotopic study. Env. Sci. Technol. 29, 1288–1296.

Doe, B.R., 1970. Lead Isotopes. Springer, Berlin.

Elbaz-Poulichet, F., Hollinger, P., Huang, W.W., Martin, J.M., 1984. Lead cycling in estuaries, illustrated by the Gironde estuary, France. Nature 308, 409–414.

Elbaz-Poulichet, F., Hollinger, P., Martin, J.M., Petit, D., 1986. Stable lead isotope ratios in major French rivers and estuaries. Sci. Tot. Env. 54, 61–76.

Erel, Y., Patterson, C.C., Scott, M.J., Morgan, J.J., 1990. Transport of industrial lead in snow through soil to stream water and groundwater. Chem. Geol. 85, 383–392.

Erel, Y., Morgan, J.J., Patterson, C.C., 1991. Natural levels of lead and cadmium in a remote mountain stream. Geochim. Cosmochim. Acta 55, 707–719.

Farmer, J.G., MacKenzie, A.B., Sudgen, C.L., Bryant, C.L., Eades, L.J., Bailey-Watts, A.E., Kirika, A., 1993. Allan, R.J., Nriagu, J.O. (Ed.). Proceedings of the Ninth International Conference on Heavy Metals in the Environment; CEP Consultants, Edinburgh, 2, pp. 211–214.

Flament, P., 1985. Les métaux traces associés aux aérosols atmosphériques: apports au milieu marin du littoral Nord-Pas de Calais. Thèse de 3ème cycle. University of Lille.

Graney, J.R., Halliday, A.N., Keeler, G.J., Nriagu, J.O., Robbins, J.A., Norton, S.A., 1995. Isotopic record of lead pollution in lake sediments from the northeastern United States. Geochim. Cosmochim. Acta 59, 1715–1728.

Grousset, F.E., Quétel, C.R., Thomas, B., Buat-Ménard, P., Donard, O.F.X., Buchet, A., 1994. Transient Pb isotopic signatures in the western European atmosphere. Env. Sci. Technol. 28, 1605–1608.

Grousset, F.E., Quétel, C.R., Thomas, B., Donard, O.F.X., Lambert, C.E., Guillard, F., Monaco, A., 1995. Anthropogenic vs lithogenic origins of trace elements (As, Cd, Pb, Rb, Sc, Sn, Zn) in water column particles: northwestern Mediterranean Sea. Mar. Chem. 48, 291–310.

Hamelin, B., Grousset, F., Sholkovitz, E.R., 1990. Pb isotopes in surficial pelagic sediments from the North Atlantic. Geochim. Cosmochim. Acta 54, 37–47.

Hamester, M., Stechmann, H., Steiger, M., Dannecker, W., 1994. The origin of lead in urban aerosols — a lead isotopic study. Sci. Tot. Environ. 146/147, 321–323.

Hamilton, E.I., Clifton, R.J., 1979. Isotopic abundances of lead in estuarine sediments, Swansea Bay, Bristol Channel. Estuarine Coast. Mar. Sci. 8, 271–278.

Hirao, Y., Mabuchi, H., Fukuda, E., Tanaka, H., Imamura, T., Todoroki, H., Kimura, K., Matsumoto, E., 1986. Lead isotope ratios in Tokyo Bay sediments and their implications in the lead consumption of Japanese industries. Geochem. J. 20, 1–15.

Keinonen, M., 1992. The isotopic composition of lead in man and the environment in Finland 1966–1987: isotope ratios of lead as indicators of pollutant source. Sci. Tot. Env. 113, 251–268.

Kramers, J.D., Tolstikhin, I.N., 1997. Two terrestrial lead isotope paradoxes, forward transport modelling, core formation and the history of the continental crust. Chem. Geol. 139, 75–110.

Monna, F., Ben, Othman D., Luck, J.M., 1995. Pb isotopes and Pb, Zn and Cd concentrations in the rivers feeding a coastal pond (Thau, southern France): contraints on the origin(s) and flux(es) of metals. Sci. Tot. Env. 166, 19–34.

Monna, F., Mathieu, D., Marques, A.N., Lancelot, J., Bernat, M., 1996. A comparison of PERALS to alpha spectrometry and beta counting: a measure of the sedimentation rate in a coastal basin. Anal. Chim. Acta 330, 107–115.

Monna, F., Lancelot, J., Bernat, M., Mercadier, H., 1997a. Taux de sédimentation dans l'étang de Thau à partir des données géochronologiques, géochimiques et des repères stratigraphiques. Oceanol. Acta 20, 627–638.

Monna, F., Lancelot, J.R., Croudace, I., Cundy, A., Lewis, J.T., 1997b. Pb isotopic signature of urban air in France and United Kingdom: Implications on Pb pollution sources. Env. Sci. Technol. 31, 2277–2286.

Őhlander, B., Ingri, J., Pontér, C., 1993. Lead isotopes as tracers of lead pollution from various sources: an example from northern Sweden. Appl. Geochem. 2, 67–70.

Péna, G., 1989. Sels nutritifs et micropolluants métalliques dans un écosystème lagunaire: l'étang de Thau. Doct. Thesis, Univers. Montpellier.

Petelet, E., Ben, Othman D., Luck, J.M., 1997. Etude des charges dissoute et particulaire dans une rivière méditerranéenne (Vène, Hérault, France): apport des éléments majeurs, traces et des isotopes du plomb et du strontium sur l'origine et la circulation des eaux et des charges transportées. C.R. Acad. Sci. Paris 324 IIa, 753–761.

Petit, D., 1974. ^{210}Pb et isotopes stables du plomb dans les sédiments lacustres. Earth Planet. Sci. Lett. 23, 199–205.

Petit, D., Mennessier, J.P., Lamberts, L., 1984. Stable lead isotopes in pond sediments as tracer of past and present atmospheric lead pollution in Belgium. Atmosph. Env. 18, 1189–1193.

Puchelt, H., Kramar, U., Clumming, G.L., Krstic, D., Nšltner, T., Schšllte, M., Schweikle, V., 1993.

Anthropogenic Pb contamination of soils, Southwest Germany. Appl. Geochem. 2, 71–73.

Ritson, P.I., Esser, B.K., Niemeyer, S., Flegal, A.R., 1994. Lead isotopic determination of historical sources of lead to Lake Erie, North America. Geochim. Cosmochim. Acta 58, 3297–3305.

Roberts, S.J., Ruiz, J., 1989. Geochemistry of exposed granulite facies terrains and lower crustal xenoliths in Mexico. J. Geophys. Res. 94, 7961–7974.

Shirahata, H., Elias, R.W., Patterson, C.C., 1980. Chronological variations in concentrations and isotopic compositions of anthropogenic atmospheric lead in sediments of a remote subalpine pond. Geochim. Cosmochim. Acta 44, 149–162.

Shotyk, W., Cheburkin, A.K., Appleby, P.G., 1996. Two thousand years of atmospheric arsenic, antimony, and lead deposition recorded in an ombrotrophic peat bog profile, Jura Mountains, Switzerland. Earth Planet. Sci. Lett. 145, 1–7.

Sudgen, C.L., Farmer, J.G., McKenzie, A.B., 1993. Isotopic ratios of lead in contemporary environmental material from Scotland. Env. Geochem. Health 15, 59–65.

Véron, A., Lambert, C.E., Isley, A., Linet, P., Grousset, G., 1987. Evidence of recent lead pollution in deep Northeast Atlantic sediments. Nature 326, 278–281.

Wahlen, M., Thompson, R.C., 1980. Pollution records from sediments of three lakes in New York State. Geochim. Cosmochim. Acta 44, 333–339.

Zwolsman, J.G., Berger, G.W., Van Eck, G.T.M., 1993. Sediment accumulation rates, historical input, postdepositional mobility and retention of major elements and trace metals in salt marsh sediments of the Scheldt estuary, SW Netherlands. Mar. Chem. 44, 73–94.